

A review and perspective on a convergence analysis of the direct simulation Monte Carlo and solution verification

R. S. Myong (명노신)^{a),1)}, A. Karchani^{b),2)}, O. Ejtehadi^{c)},

^{a)}School of Mechanical and Aerospace Engineering, Gyeongsang National University, Jinju, South Korea

^{b)}ANSYS Inc., Lebanon, NH, US

^{c)}Supercomputing Modeling and Simulation Center, Korea Institute of Science and Technology Information (KISTI), Daejeon, South Korea

Abstract:

In 1963, G. A. Bird published a research note on his investigation of a rigid sphere gas reaching translational equilibrium using a Monte Carlo type method. Since then, the method has been developed into a primary workhorse to computationally solve the Boltzmann kinetic equation. As it is increasingly applied to challenging problems in the real world, verification studies of the method have become a critical issue. In this paper, we review previous studies on this challenging subject and present a perspective on a convergence analysis of the direct simulation Monte Carlo (DSMC) method and solution verification. During this process, a verification method based on the physical laws of conservation is studied in depth. In particular, a convergence history plot on all three types of computational errors—decomposition, statistical, and round-off—is presented for two benchmark problems. Finally, future research topics to maximize the full potential of the DSMC method, pioneered by the late G. A. Bird, are suggested.

Keywords: Direct simulation Monte Carlo; verification; computational error; convergence; error estimation.

¹⁾ Corresponding author: Tel: +82-55-772-1645. Email: myong@gnu.ac.kr.

²⁾ Formerly research assistant at School of Mechanical and Aerospace Engineering, Gyeongsang National University, Jinju, South Korea.

I. Introduction

In May 1963, G. A. Bird submitted a research note of two pages to the *Physics of Fluids* journal on the investigation of a rigid sphere gas reaching translational equilibrium using a Monte Carlo type method (and the Silliac digital computer)¹. In the note, he demonstrated the method was sufficiently economical in its computing time and storage requirements. Indeed, his method turned out to be a significant step towards developing a probabilistic mesoscopic simulation method, which was at that time a drastic departure from the then-dominant deterministic microscopic molecular dynamics (MD), which explicitly computes the simultaneous equations of all the molecules.

Since then, the method, now called DSMC (direct simulation Monte Carlo)^{2,3}, has been developed into a primary workhorse to computationally solve the Boltzmann or equivalent kinetic equations, and is routinely being applied to various flow problems of scientific and technological interest, including rarefied hypersonic gas flows^{4,5}, micro- and nano-scale gases^{6,7}, and hydrodynamic flows^{8,9}.

However, as is common when new computational models are increasingly applied to real world (application) problems, verification and validation of the new models become critical practical issues¹⁰. The failure to adequately perform verification can lead to incorrect assessment of the validity of the computational model, and can result in computational errors being calibrated into the supposedly-accurate physical model.

The verification and validation issues¹⁰ have been studied very actively in recent years, in particular, in the computational fluid dynamics (CFD) community, which works to develop various numerical methods for partial differential equations governing the macroscopic motion of fluids¹⁰⁻¹². For verification of computational algorithm—concerning mainly the accuracy of the computational solution to the given mathematical model of the system—several well-known methods have been developed to evaluate computational errors. These

include the order of accuracy test using an exact solution, convergence test, discretization error quantification, and code-to-code comparison.

Among these methods, the order of accuracy test is the most rigorous, and several methods have been developed to obtain exact solutions for the test. The traditional methods are based on analytical solutions in a closed function using only elementary and special functions and approximate solutions like infinite series solutions. A more recent method is the so-called method of manufactured solutions in which the exact solutions are obtained to the modified governing equations made up of original equations and source terms.

For the verification of solutions, the main focus is the estimation of various computational errors that inevitably occur when solving a mathematical model computationally. The sources of computational errors can be categorized into discretization of computational domain and boundary, iterative routine, and round-off. To estimate discretization error, there are several methods available, like recovery methods based on mesh refinement and residual (and truncation) error-based methods.

On the other hand, it is not clear how to apply these verification methods to the DSMC method, since the DSMC method is not based on any partial differential equations. The DSMC method directly simulates the molecular behavior of gases by decomposing the motion of the particles into two steps—deterministic movement and stochastic collision via Monte Carlo—with the assumption of one simulated particle representing a large number of real particles. Therefore, a considerable portion of the aforementioned verification methods developed for partial differential equations in the CFD community may not be applicable to the DSMC method. A similar challenge may be present in other pure simulation methods, like MD¹³.

One vital difference between the DSMC method and the CFD method is the stochastic nature of the algorithm. The DSMC method inherits the statistical features of the probabilistic

methods, such as random fluctuation and statistical uncertainty. Moreover, a probability sampling process is needed to filter out the statistical uncertainty. As a result, computational errors in the DSMC method can be categorized into three types; decomposition (or discretization), statistical, and round-off errors. The three types of error and associated computational parameters of the DSMC method are depicted in Fig. 1.

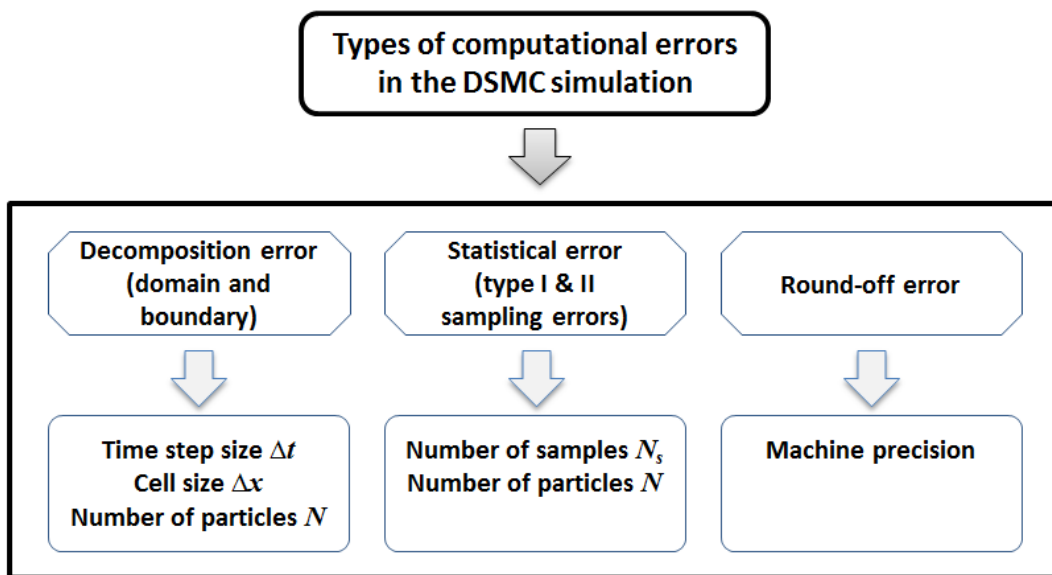


Fig. 1. Types of computational errors in the DSMC simulation

The decomposition error arises mainly from the finiteness of time step size, cell size, and number of particles within a cell, in the computational domain, and a boundary treatment of an inherently approximate nature. The statistical error is generated due to the stochastic nature of the DSMC method. The statistical error associated with the sampling procedure can be further categorized as type I (an incorrect rejection of samples belonging to the steady state—premature stopping of sampling) and type II (an incorrect acceptance of samples not belonging to the steady state—premature initiation of sampling). Lastly, machine error, the so-called round-off-error, is inevitable in any computational method.

In this paper, we aim to review previous studies on this challenging subject and present a perspective on convergence analysis of the DSMC method and solution verification. During this process, a verification method of the DSMC method based on the physical laws of conservation is studied in depth. In particular, a convergence history plot on all three types of computational errors—decomposition, statistical, and round-off—for three measures (mass, momentum, and energy) is presented for two benchmark problems, boundary-driven Couette flow and boundary-free shock structure.

II. Convergence of DSMC to the Boltzmann kinetic equation

The DSMC method directly simulates the motion and interaction of statistically representative particles, as opposed to real particles in MD, rendering it a mesoscale method. In this context, a question was naturally raised in the 1970's and 80's about how the DSMC method is related to the Boltzmann kinetic equation; specifically, whether the DSMC solution can be proven mathematically to converge to the solution of the Boltzmann kinetic equation of a gas undergoing binary collisions between gas particles.

In a series of papers^{14,15}, Nanbu proved that his Monte Carlo method, even though computationally very expensive, will converge to the solution of the Boltzmann kinetic equation. He also showed that, among all the available Monte Carlo methods, including the DSMC method, his method is the only one for which the convergence to the Boltzmann kinetic equation can be mathematically proved.

Babovsky and Illner¹⁶ developed a method to prove the convergence of Nanbu's method under certain conditions. Wagner¹⁷ applied the method to the DSMC method and proved theoretically that the DSMC solution will converge to the solution of the Boltzmann kinetic equation, if the computational parameters are chosen properly (and when no wall surface boundary condition is involved in the simulation). In passing, it must be noted that the

Boltzmann kinetic theory has not been fully worked out to modify the collision term that should correctly reflect the molecular collision with the wall surface atoms.

III. Convergence analysis for verification of the DSMC method

CFD methods based on deterministic partial differential equations can naturally report the run-time residual, to examine stability and error behaviors. On the other hand, there is less interest in checking instability in the DSMC method, since it never exhibits instability during simulation. Nonetheless, measuring and reporting the amount of computational errors at every simulation step remains crucial in the DSMC method as well. The convergence history plot should be able to describe the contribution of various error sources during the simulation.

Several benchmark flow problems were proposed for the convergence analysis of the DSMC method in the past. They are the Fourier flow driven by temperature difference, the Couette flow driven by wall velocity shear, the boundary-free shock structure, and external flow past a circular cylinder, as illustrated in Fig. 2.

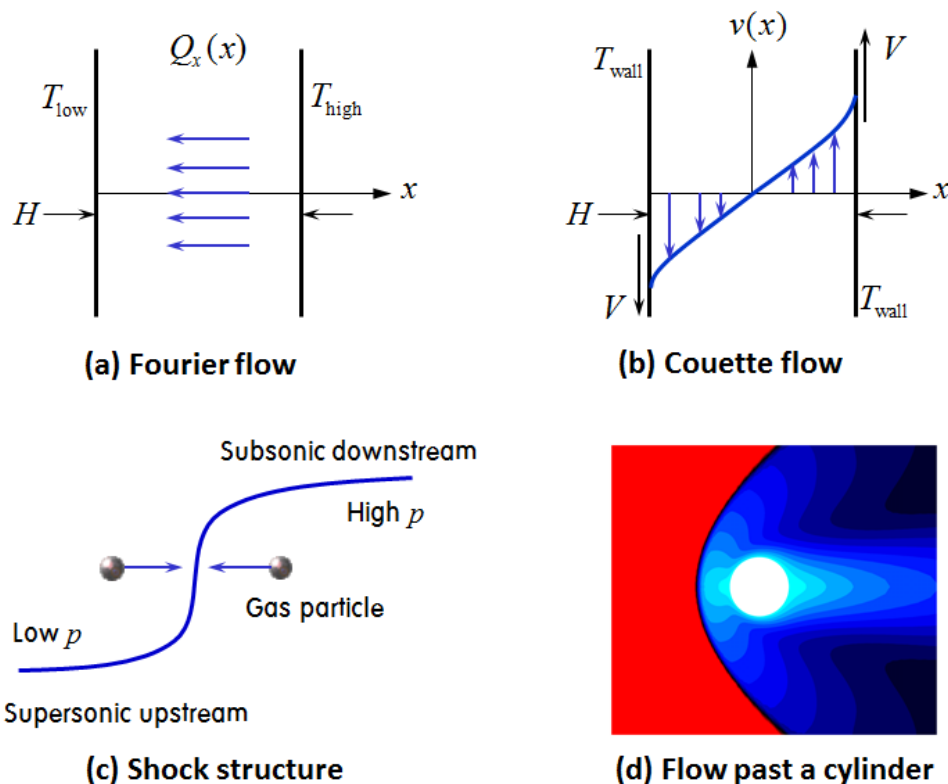


Fig. 2. The schematic of the benchmark problems: (a) the Fourier flow driven by temperature difference, (b) the Couette flow driven by wall velocity shear, (c) the boundary-free shock structure, and (d) external flow past a circular cylinder.

Many studies have been conducted to investigate the effects of computational parameters and the quantification of computational errors associated with them. Meiburg¹⁸ compared the MD and the DSMC methods with respect to the capability of simulating vorticity after solving flows around simple geometries. He showed that the time-step size and the number of particles per cell in the DSMC method need to be examined more carefully in order to yield accurate results. Alexander *et al.*¹⁹ investigated the dependence of the transport coefficients on the cell size in the DSMC method in order to analyze the role of cell-size on decomposition error. They found that the error comes from the collision pair selection division where particle partners are selected from any place throughout the collision cell.

Garcia and Wagner²⁰ investigated the effects of time-step size on the accuracy of the transport coefficient (viscosity, thermal conductivity, and self-diffusion). They found that the time-step size error is closely connected to re-collision phenomena. They also demonstrated the second-order accuracy of time-step size truncation error in the DSMC algorithm. Hadjiconstantinou²¹ derived an explicit expression for describing the influence of time-step size on the decomposition error. Gallis *et al.*²² showed that the DSMC solutions agreed well with the continuum solutions of Chapman–Enskog (CE) and the moment-hierarchy (MH) method at small and finite Knudsen numbers. Bird²³ estimated the steady state convergence on the basis of the variation in the total number of simulated particles (i.e., the Boltzmann collisional invariant on the mass) throughout the simulation domain. Bird *et al.*²⁴ and Gallis *et al.*²⁵ investigated the accuracy and convergence of the sophisticated DSMC algorithm—developed with the aim of increasing computational efficiency—by comparing the solutions with the exact solution of the Boltzmann equation for one-dimensional Fourier-Couette flow. It was shown that the sophisticated DSMC algorithm can predict transport properties and

Sonine polynomial coefficients with good agreement with their corresponding infinite-approximation Chapman–Enskog theoretical values. They also characterized the convergence of the new algorithm in a three-dimensional implementation.

Burt and Boyd²⁶ introduced convergence criterion based on the variation of particle fluxes on the boundaries at two successive time-steps in order to study weak transient behavior in small regions of relatively low density or recirculating flows. Karchani and Myong²⁷ presented the first convergence analysis of all computational errors in the DSMC method. They quantified the errors of the DSMC method using a measure based on the strict conservation of mass, momentum and energy. Unlike previous methods that targeted only one type of error, the method was shown to be able to take all three computational errors into account. Taheri *et al.*²⁸ provided an analysis of the convergence behavior of the simplified Bernoulli-Trial (SBT) collision scheme in the DSMC framework using a similar approach which has been applied by Gallis *et al.*^{22,29}. Akhlaghi *et al.*³⁰ investigated the Fourier heat transfer problem at the early slip regime and found that, in addition to collision frequency and collision separation distance, the level of repeated collisions plays a critical role in the accuracy of the heat flux prediction in the DSMC method.

IV. Convergence analysis based on the physical laws of conservation

A. Physical laws of conservation

The physical conservation laws can be written in the integral form:

$$\frac{\partial}{\partial t} \int_V \begin{bmatrix} \rho \\ \rho \mathbf{u} \\ \rho E \end{bmatrix} dV + \oint_S \begin{bmatrix} \rho \mathbf{u} \\ \rho \mathbf{u} \mathbf{u} + p \mathbf{I} + \mathbf{\Pi} \\ (\rho E + p) \mathbf{u} + \mathbf{\Pi} \cdot \mathbf{u} + \mathbf{Q} \end{bmatrix} \cdot \mathbf{n} dS = 0 \quad (4.1)$$

where S represents the surface bounding around the control volume V with unit normal vector \mathbf{n} . There are two different sets of macroscopic variables in the conservation laws; the conserved variables $(\rho, \rho\mathbf{u}, \rho E)$ and the non-conserved variables $(\mathbf{\Pi}, \mathbf{Q})$, where ρ is the density, \mathbf{u} is the average bulk velocity vector, E is the total energy density, and $\mathbf{\Pi}, \mathbf{Q}$ represent the shear stress tensor and the heat flux vector, respectively.

It can be proved that the physical conservation laws (4.1) are the exact consequence of the Boltzmann kinetic equation. Only after some approximations like the linear Navier and Fourier (or the first-order Chapman-Enskog in kinetic theory terms) constitutive relations are introduced to the shear stress and the heat flux in (4.1), they become approximate, thereby valid only at not-far-from-thermal-equilibrium.

In fact, the conservation laws (4.1) can be derived directly from the following Boltzmann kinetic equation of the distribution function f ,

$$\frac{\partial f}{\partial t} + \mathbf{v} \cdot \nabla f = C[f, f_2], \quad (4.2)$$

where \mathbf{v} is the particle velocity and the term $C[f, f_2]$ represents the Boltzmann collision integral of the binary interaction among the particles. For the conservation law of momentum, differentiating the statistical definition of the momentum with time and combining with the Boltzmann kinetic equation yield²⁷

$$\frac{\partial}{\partial t} \langle m\mathbf{v}f \rangle = \left\langle m\mathbf{v} \frac{\partial f}{\partial t} \right\rangle = -\langle m(\mathbf{v} \cdot \nabla f) \mathbf{v} \rangle + \langle m\mathbf{v}C[f, f_2] \rangle.$$

Then the first term on the right-hand side becomes ($\mathbf{v} = \mathbf{u} + \mathbf{c}$)

$$-\langle m(\mathbf{v} \cdot \nabla f) \mathbf{v} \rangle = -\nabla \cdot \langle m\mathbf{v}\mathbf{v}f \rangle = -\nabla \cdot \{ \rho\mathbf{u}\mathbf{u} + \langle m\mathbf{c}\mathbf{c}f \rangle \}.$$

Here the symbols \mathbf{c} and $\langle \rangle$ denote the particle velocity and the integral in velocity space, respectively. After the decomposition of stress \mathbf{P} into the hydrostatic pressure p and the viscous shear stress $\mathbf{\Pi}$ ($[\]^{(2)}$ denoting the traceless symmetric part of the tensor),

$$\mathbf{P} \equiv \langle m\mathbf{c}\mathbf{c}f \rangle = p\mathbf{I} + \mathbf{\Pi} \text{ where } p \equiv \langle m\text{Tr}(\mathbf{c}\mathbf{c})f / 3 \rangle, \mathbf{\Pi} \equiv \langle m[\mathbf{c}\mathbf{c}]^{(2)} f \rangle,$$

and, using the collisional invariance of the momentum, $\langle m\mathbf{v}C[f, f_2] \rangle = 0$, we obtain

$$\frac{\partial(\rho\mathbf{u})}{\partial t} + \nabla \cdot (\rho\mathbf{u}\mathbf{u} + p\mathbf{I} + \mathbf{\Pi}) = 0,$$

which is nothing but the second equation of the conservation laws (4.1). Owing to this exact equivalence, the physical conservation laws (4.1) can be utilized to verify numerical solutions of the Boltzmann kinetic equation and the DSMC method.

B. Convergence history of boundary-driven Couette flow problem

The Couette flow is defined as the flow confined between two infinite, parallel, flat plates at $x = \pm H/2$ driven by the shear motion of one or both of the plates in opposite directions with constant velocity, while the temperature of the walls remains constant. The fluid is assumed to be steady state without any external forces and to move in the y -direction only, as shown in Fig. 2(b). Therefore, this shear-driven flow problem is an excellent benchmark case for studying the accuracy of the DSMC method, including the effects of the solid wall boundary condition. In this flow problem, the conservation laws (4.1) are greatly reduced: still exact to the original Boltzmann kinetic equation,

$$\frac{d}{dx} \begin{bmatrix} 0 \\ p + \Pi_{xx} \\ \Pi_{xy} \\ \Pi_{xz} \\ \Pi_{xy} v + Q_x \end{bmatrix} = 0 \Rightarrow \begin{aligned} p + \Pi_{xx} &= C_1 \\ \Pi_{xy} &= C_2 \\ \Pi_{xz} &= C_3 \\ \Pi_{xy} v + Q_x &= C_4 \end{aligned} \quad (4.3)$$

where $C_{1,2,3,4}$ are integration constants representing conservative values, since they remain constant throughout the simulation domain. The errors associated with the conservation laws can then be defined as follows²⁷:

$$\begin{aligned}
\text{error}_{x\text{-momentum}} &\equiv p + \Pi_{xx} - \left[\overline{p + \Pi_{xx}} \right] \\
\text{error}_{y\text{-momentum}} &\equiv \Pi_{xy} - \overline{\Pi_{xy}} \\
\text{error}_{z\text{-momentum}} &\equiv \Pi_{xz} - \overline{\Pi_{xz}} \\
\text{error}_{\text{energy}} &\equiv \Pi_{xy} v + Q_x - \left[\overline{\Pi_{xy} v + Q_x} \right] \\
\text{error}_{EOS} &\equiv p - \rho RT \quad \Rightarrow \text{Round-off error}
\end{aligned} \tag{4.4}$$

where the symbol $\bar{\square}$ denotes reference values of conservative values \square and they can be calculated based on the average values of the macroscopic properties in the whole domain. Flows studied in current work are steady state and, hence, the microscopic properties are just sampled once at each time step. All macroscopic properties—both conserved and non-conserved—can be computed in a DSMC simulation on the fly using the sampled microscopic information. Then, the reference value can be computed at a reference location in the domain (e.g., center of the channel in the present flow problem). Finally, the error values are determined in each sample cell and the L_2 error norms are computed at each time step.

In Fig. 3, the complete convergence history of the DSMC solution based on the physical laws of conservation (4.4) is plotted²⁷. It should be mentioned that, to the best knowledge of the authors, no attempt has been made in the past to apply a verification strategy based on conservation laws developed in CFD to the simulation methods like DSMC and produce very instructive convergence results like Fig. 3 of all conserved variables. Two diffuse walls having constant temperature (293 K) are moving in opposite directions with constant velocity corresponding to Mach number 1 (relative Mach number two). A representative monatomic gas (molecular diameter 4×10^{-10} meter and molecular mass 6.64×10^{-26} kg) was assumed. The Knudsen number based on the gap between walls was set to be 1.0. The values of $\Delta t = 0.01\tau_\infty$, $\Delta x = 1/32\lambda_\infty$, $N_S = 10^8$ were used for time-step, cell-size, and the number of sample steps, respectively, for four different numbers of particles per cell (40, 80, 160, 320).

The convergence behavior of the conservation laws of x,y -momentum and energy is composed of two separate phases. In the first phase, the statistical error is dominant and the total error decreases quickly with increasing sample size. This phase continues until the number of sample steps reaches certain values, when the contribution of the statistical error to total error becomes negligible. Furthermore, the rate of this decrease is inversely proportional to the square root of the sample steps ($1/\sqrt{N_s}$).

The second phase starts when the combination of decomposition and boundary condition errors becomes prominent, in comparison with the statistical error. The decomposition and boundary condition errors do not decrease with increasing sample size, since these errors do not depend on sample steps. The decomposition error can be changed by adjusting the physical parameters, like time-step size. Owing to the presence of these errors, the total error converges to a finite constant value, even when a large number of samples, or particles, is used. In other words, more particles can result in a faster convergence rate for the statistical part, but this would not change the decomposition and boundary condition errors.

On the other hand, the statistical error in the z -momentum equation does not converge to any constant value; it still declines, even after more than 10^8 samples. A possible explanation for this behavior is that the z -spatial coordinate does not contribute to locating the particles in the cells and selecting the collision pairs in the present 1D-Coutte flow problem. Therefore, the convergence rate of the z -momentum error will follow the statistical error pattern and flatten after reaching the limit of round-off error. Lastly, the round-off error may be observed by examining error values for the equation of state. The values show the maximum limit of accuracy of the current simulation, and that it is not changed by increasing sample steps or number of particles.

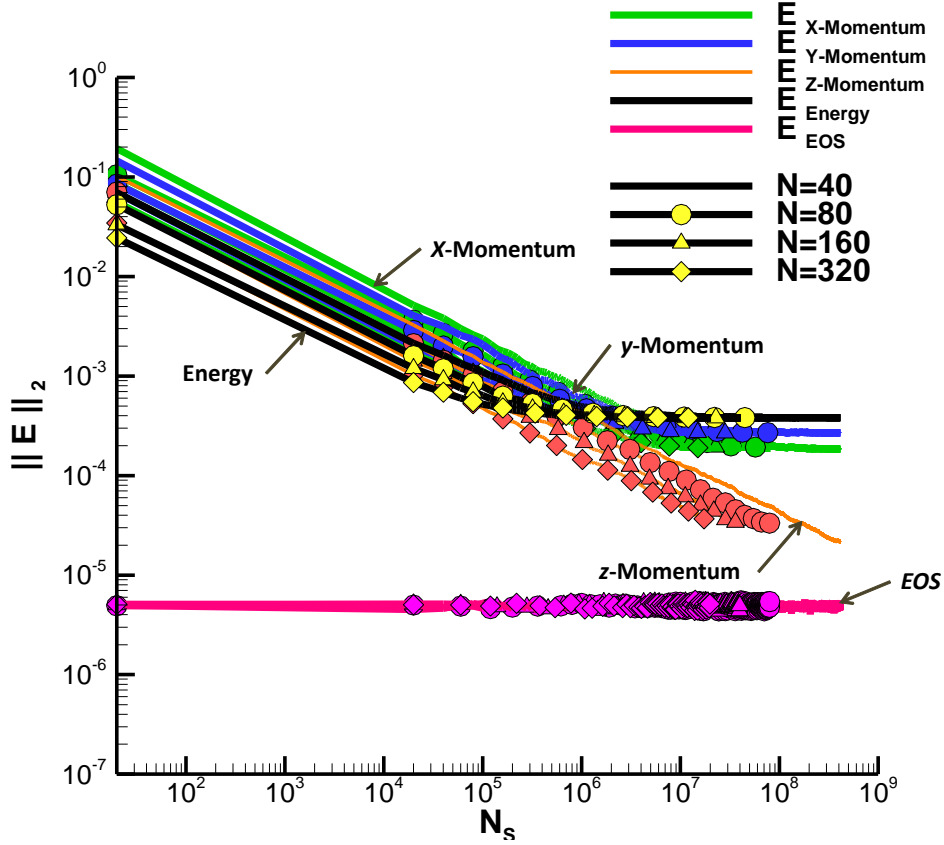


Fig. 3. The convergence history for conservation laws and the equation of state for different numbers of particles in the Couette flow problem. The vertical axis shows the order of magnitude of the normalized error based on the two-norm L_2 . Reproduced with permission from Comput. Fluids **115**, 98 (2015). Copyright 2015 Elsevier.²⁷

C. Decomposition errors in the boundary-free shock structure problem

The stationary shock wave structure is a pure one-dimensional compressive gas flow defined as a very thin (order of mean free path) stationary gas flow region between the supersonic upstream and subsonic downstream, as shown in Fig. 2(c). Due to absence of the boundary condition, it allows to study the inherent behavior of a simulation method free from the contamination caused by the boundary condition. In this problem, the conservation laws (4.1) are reduced as follows: still exact to the original Boltzmann kinetic equation,

$$\frac{d}{dx} \begin{bmatrix} \rho u \\ \rho u^2 + p + \Pi_{xx} \\ \Pi_{xy} \\ \Pi_{xz} \\ (\rho E + p)u + \Pi_{xx}u + Q_x \end{bmatrix} = 0 \Rightarrow \begin{aligned} \rho u &= C_1 \\ \rho u^2 + p + \Pi_{xx} &= C_2 \\ \Pi_{xy} &= C_3 \\ \Pi_{xz} &= C_4 \\ (\rho E + p)u + \Pi_{xx}u + Q_x &= C_5 \end{aligned} \quad (4.5)$$

where $C_{1,2,3,4,5}$ are again integration constants. Then, the errors associated with the conservation laws may be defined at each sample cell in the simulation domain as²⁷:

$$\begin{aligned} \text{error}_{mass} &\equiv \rho u - \overline{\rho u} \\ \text{error}_{x\text{-momentum}} &\equiv \rho u^2 + p + \Pi_{xx} - \overline{\rho u^2 + p + \Pi_{xx}} \\ \text{error}_{y\text{-momentum}} &\equiv \Pi_{xy} - \overline{\Pi_{xy}} \\ \text{error}_{z\text{-momentum}} &\equiv \Pi_{xz} - \overline{\Pi_{xz}} \\ \text{error}_{energy} &\equiv (\rho E + p)u + \Pi_{xx}u + Q_x - \overline{(\rho E + p)u + \Pi_{xx}u + Q_x} \\ \text{error}_{EOS} &\equiv p - \rho RT \quad \Rightarrow \text{Round-off error} \end{aligned} \quad (4.6)$$

In the present shock structure problem containing stiff shock regions, it is not clear how to select a reference location in the domain to obtain the reference value. To resolve this problem, the reference values are evaluated first in each sample cell and then averaged in the whole computation domain.

Time-step size, cell size, and number of particles are critical computational parameters which affect the decomposition errors in the DSMC method. In order to investigate decomposition errors, the shock structure problem of a hard sphere with upstream Mach numbers of 2.0 and 10.0 is considered. Cell size, number of particles per cell, and the number of sample steps ($\Delta x = 1/16\lambda_\infty$, $N = 160$, $N_S = 10^8$) are used for three different time-step sizes $\Delta t / \tau_\infty = 1.0, 0.1, 0.01$.

The time-step size, Δt , is the most important computational parameter, since it plays an essential role in decoupling the movement and collision steps in the DSMC method. The

measured errors based on deviations from conservation laws are shown in Figs. 4 and 5. The normalized errors associated with conservation laws were shown to remain mostly constant throughout the domain and to decrease with the decreasing time-step size. However, notable hikes were found at the shock transition region at the center for conservation laws of mass, x -momentum, and energy. These hikes were amplified with increasing time-step size, in particular, for the large value $\Delta t / \tau_\infty = 1.0$. Furthermore, the largest normalized errors are found in the x -momentum conservation and remain noticeable even for small time-step sizes as low as $\Delta t / \tau_\infty = 0.01$.

The hikes in the x -momentum error may be related to there being insufficient collisions between particles to maintain local equilibrium in the stiff shock region, since the macroscopic properties vary in the scale of the local mean free path. In addition, the high degree of non-equilibrium and the reduced local mean collision time inside the shock region may ultimately cause higher x -momentum error. Hence, in order to reduce the decomposition error in this region, proper cell-size and, in particular, small time-step size may be required.

When the effect of Mach number on the decomposition error is examined from Figs. 4 and 5, the normalized errors are shown to increase as the free-stream Mach number increases. The range of error hikes also increases, coinciding with the well-known shock physics, that is, that the shock thickness grows with increasing Mach number. Interestingly, a noticeable increase in errors in the downstream is observed for conservation laws of y, z -momentum in the case of $M=10$ in Figs. 5(c) and 5(d). A possible explanation is that the errors are enhanced in the downstream of the stronger shocks with much lower velocity compared to the upstream.

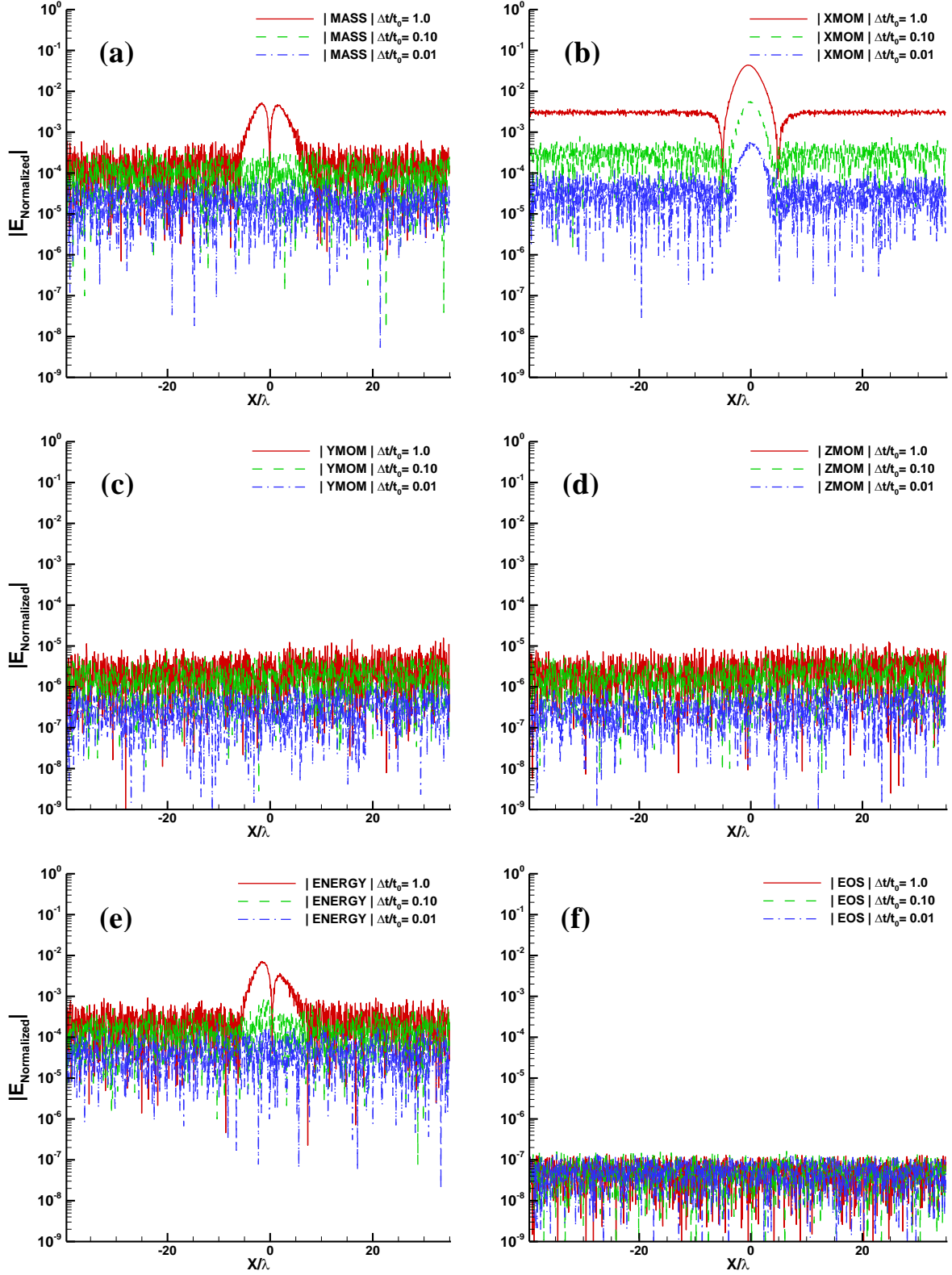


Fig. 4. The effect of time-step size on the percentage of normalized errors in the shock structure problem (Mach 2): **(a)** mass, **(b)** x -momentum, **(c)** y -momentum, **(d)** z -momentum, **(e)** energy conservation law and **(f)** equation of state. (Hard Sphere, $\Delta t = 0.01\tau_{\infty}$, $\Delta x = 1/16\lambda_{\infty}$, $N = 160$, $N_S = 10^8$)

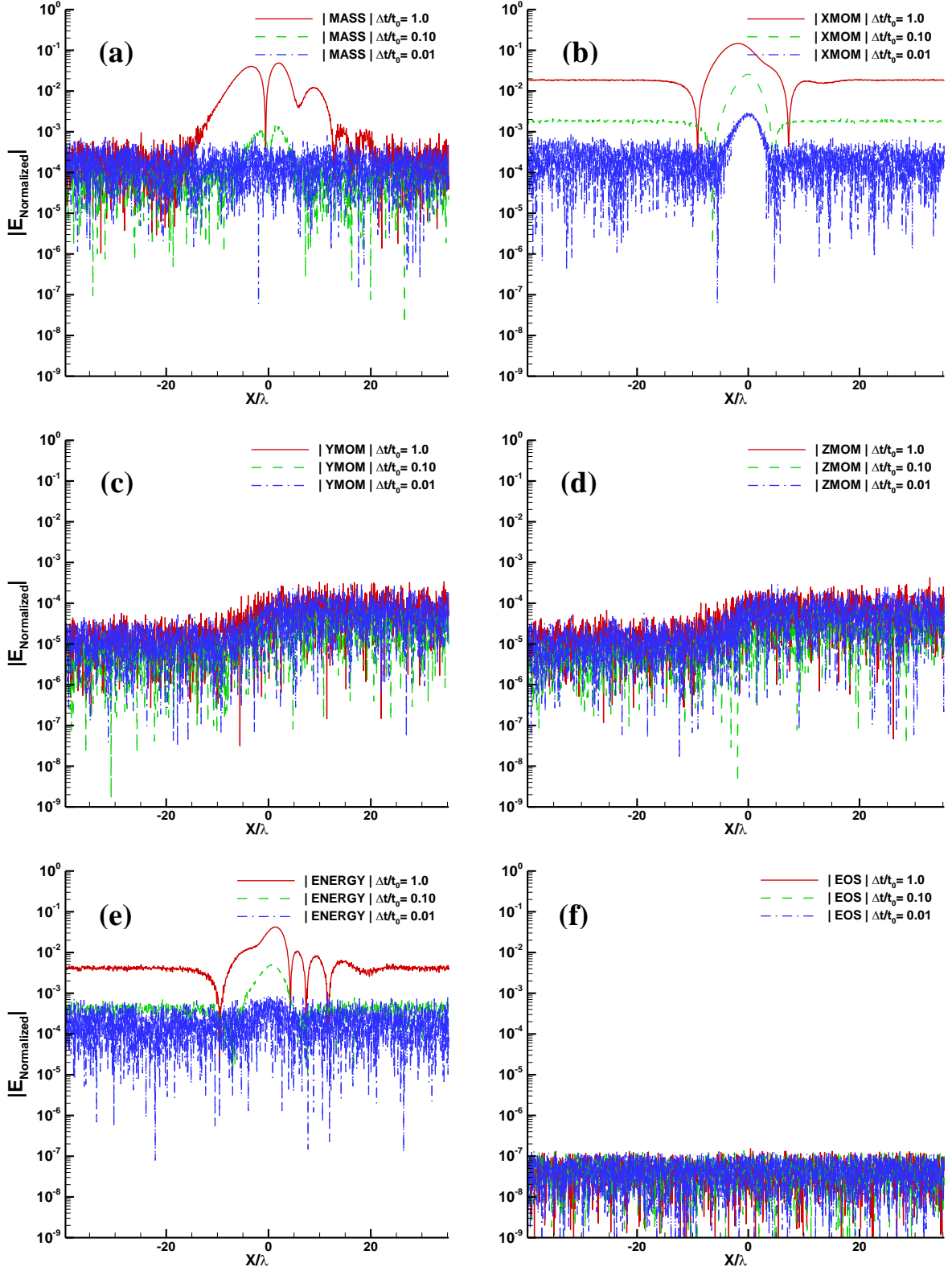


Fig. 5. The effect of time-step size on the percentage of normalized errors in the shock structure problem (Mach 10): **(a)** mass, **(b)** x -momentum, **(c)** y -momentum, **(d)** z -momentum, **(e)** energy conservation equations and **(f)** equation of state. (Hard Sphere, $\Delta t = 0.01\tau_{\infty}$, $\Delta x = 1/16\lambda_{\infty}$, $N = 160$, $N_S = 10^8$)

In order to investigate the effect of Mach number in more detail, the shock structure profiles of temperature are plotted in Fig. 6. It can be seen that the shock profile of higher Mach number ($M=10$) is more sensitive to the time-step than that of lower Mach number ($M=2$). The simulation solutions with larger time-step sizes are shown to yield overly smoothed shock profiles, in particular, near the downstream, probably due to excessive numerical viscosity rather than to actual physical viscosity caused by the larger time-step. Interestingly, a local extremum is observed in the beginning of the region downstream from the solutions of Mach number 10, obtained by fine time-steps ($\Delta t / \tau_\infty = 0.1, 0.01$). All these properties contribute to the increase in errors for higher Mach number flows.

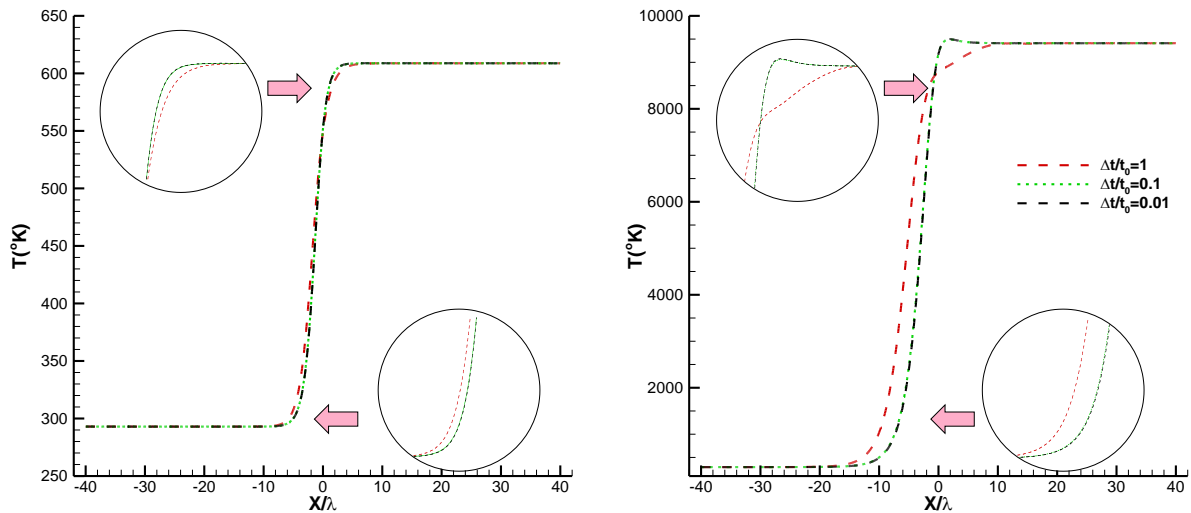


Fig. 6. Temperature profiles across the shock structure for different Mach numbers and time-step sizes: $M=2$ (left), $M=10$ (right).

The effects of time-step size, cell size, number of particles per cell on the percentage of the relative decomposition errors are summarized in Figs. 7-12. Figs. 7 and 8 show that the error is much greater in the momentum conservation laws than in the other laws for all Δt . In addition, all relative errors fall rapidly, indicating the critical role of time-step size on the decomposition error in the DSMC method. Figs. 9 and 10 show that, similar to the previous

case, the error is much greater in the momentum conservation laws than in the other laws for most of Δx . However, the change in errors is not as drastic as the previous case, implying the reduced role of cell size on the decomposition error, at least, in the range considered in the present study.

Figs. 11 and 12 indicate that the error in the momentum conservation law is in general much greater than that of the other laws. And the error in the momentum conservation laws decreases very slowly with the increasing number of particles. On the other hand, the errors in mass and energy conservation laws decrease rapidly and then flatten off, implying the number of particles play an important role in the error, and the existence of an asymptotic value, respectively. Finally, all these properties remain essentially the same for both Mach numbers (2 and 10).

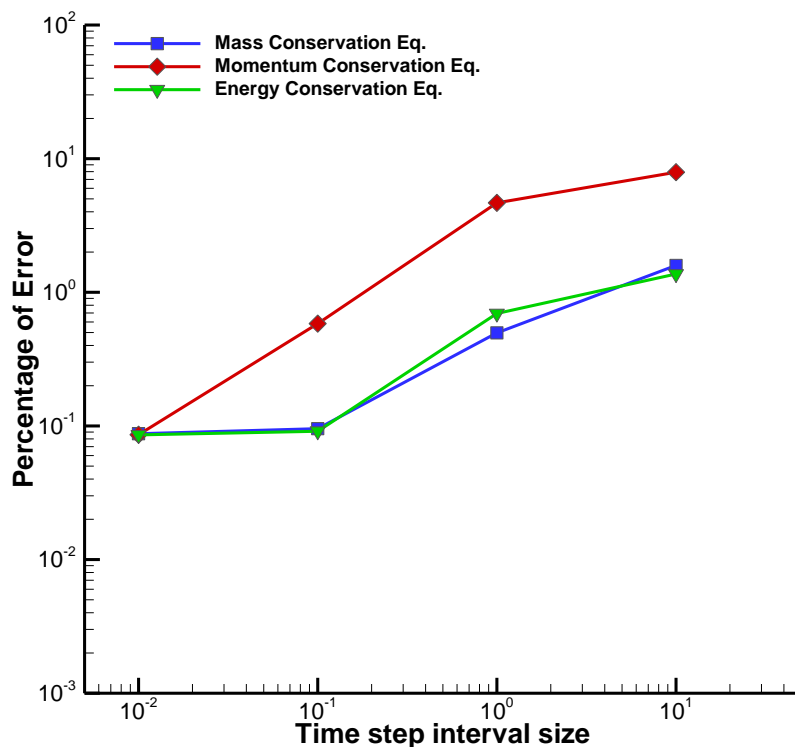


Fig. 7. The percentage of the relative errors in the DSMC solution of shock structure problem for different time-step sizes (Mach 2).

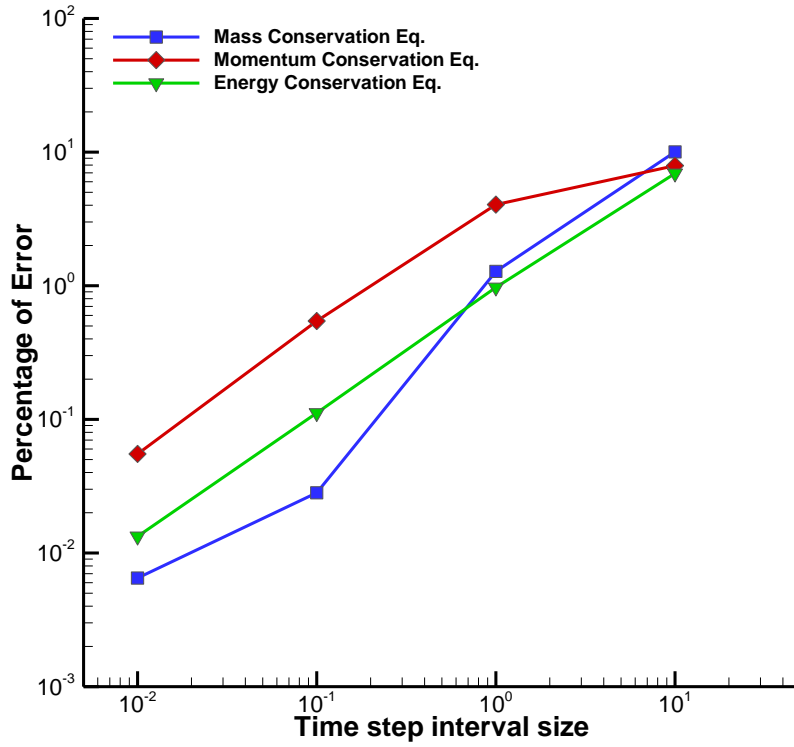


Fig. 8. The percentage of the relative errors in the DSMC solution of shock structure problem for different time-step sizes (Mach 10).

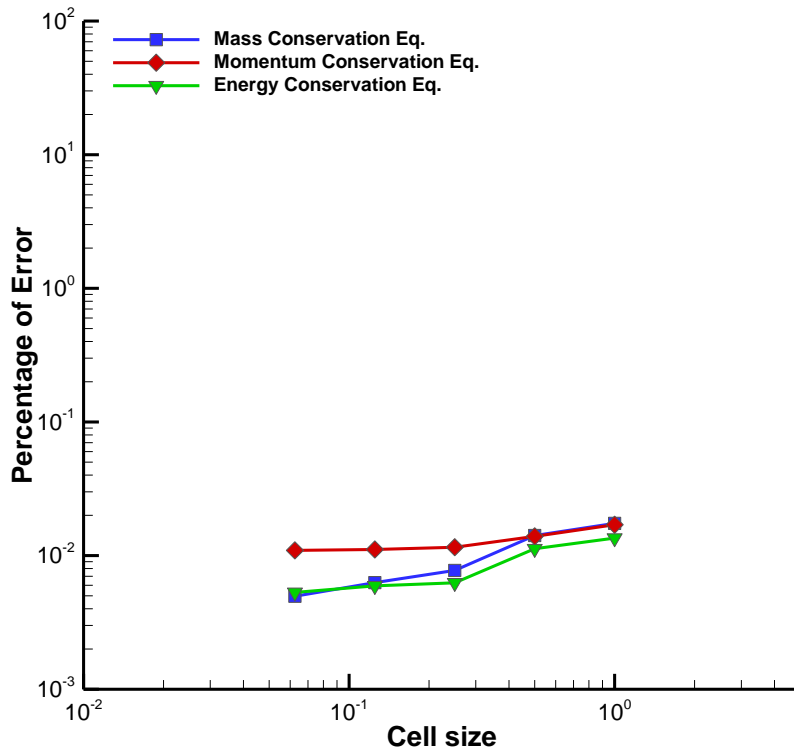


Fig. 9. The percentage of the relative errors in the DSMC solution of shock structure problem

for different cell sizes (Mach 2).

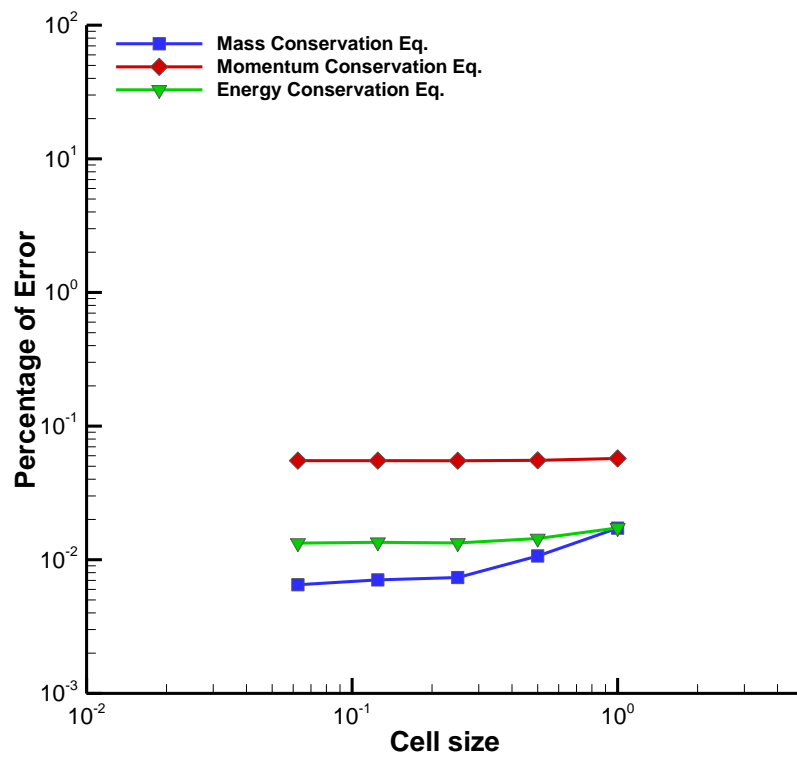


Fig. 10. The percentage of the relative errors in the DSMC solution of shock structure problem for different cell sizes (Mach 10).

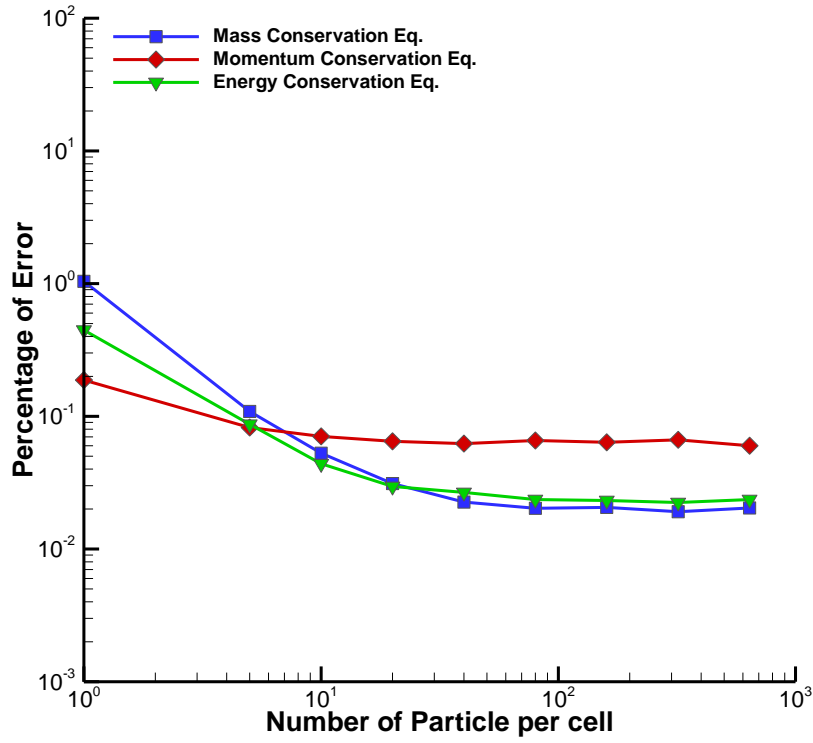


Fig. 11. The percentage of the relative errors in the DSMC solution of shock structure problem for different numbers of particles per cell (Mach 2).

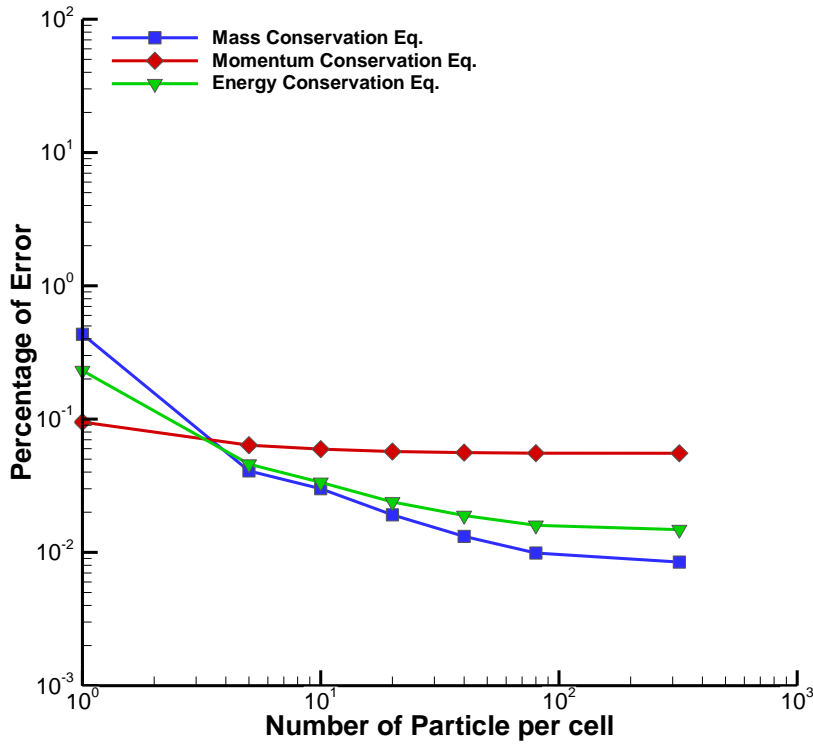


Fig. 12. The percentage of the relative errors in the DSMC solution of shock structure problem for different numbers of particles per cell (Mach 10).

V. Statistical error analysis

Among the three computational errors, the statistical error is unique to the DSMC method, which is built upon the stochastic Monte Carlo algorithm. The standard deviation and bias are major components of the statistical errors arising from random fluctuation and statistical uncertainty. There are additional sources in the statistical errors when the mean values of stochastic variables are evaluated by a sampling procedure during the simulation. They can be categorized as type I, caused by an incorrect rejection of samples belonging to the steady state (premature stopping), and type II, caused by an incorrect acceptance of samples not belonging to the steady state (premature initiation).

A. Type I incorrect rejection error: premature stopping of sampling

Garcia³¹ studied the thermodynamic fluctuations in a dilute gas under a constant heat flux in the DSMC framework and qualitatively compared the results with the previous fluctuating hydrodynamics calculation for liquids. Fallavollita *et al.*³² numerically investigated the dependence of the DSMC statistical error on the sample size for the case of independent realization in steady flow problems. However, they did not provide answers regarding the differences introduced by more complex geometries in the simulated gas, a root mean square (*rms*) error specific to a particular cell as opposed to a single measure for an entire simulation, and the effect of varying cell size.

Chen and Boyd³³ analyzed the statistical error associated with the DSMC method by employing an *rms* error as an indicator of the level of the statistical fluctuations to estimate the minimum number of particles and a maximum number of sampling steps for efficient computational simulations. The error was defined based on the reference solution obtained by the largest number of particles and the longest time-averaging. They also proposed a range of

an appropriate number of particles for minimum statistical error for a fixed computational cost.

Rjasanow *et al.*³⁴ obtained theoretical error bounds and showed that the order of convergence with respect to the particle number n was n^{-1} . They also presented ideas regarding the reduction of the number of particles in stochastic particle methods. Hadjiconstantinou *et al.*³⁵ examined the dependence of the statistical error due to finite sampling in the presence of thermal fluctuations on flow parameters such as Mach number, Knudsen number, and number of particles. They also obtained expressions for the magnitude of statistical errors due to thermal fluctuations or typical flow parameters of interest such as velocity, density temperature, and pressure.

Cave *et al.*³⁶ investigated an unsteady sampling routine for a general parallel DSMC method developed for the simulation of time-dependent flow problems in the near continuum range. They developed a post-processing procedure to improve the statistical scatter in the results while minimizing both memory and simulation time. Sun *et al.*³⁷ proposed two techniques (a direct sampling approach and a transformation to improve the acceptance rate in the acceptance-rejection method) to speed up the sampling processes in the DSMC algorithm.

Plotnikov and Shkarupa³⁸ considered the Fourier flow driven by temperature difference and constructed asymptotic confidence intervals for the statistical errors of the estimates for the three basic macro-parameters of the gas flow—density, velocity, and temperature, with the help of the central limit theorem for Markov process. Plotnikov and Shkarupa³⁹ also proved that the inter-dependence of the estimates at adjacent time-steps has a significant effect on the statistical error value. The concept of sparse samples (application of different time-steps for collision simulation and information sampling) was also introduced. The optimal relations between the sampling steps, the number of sampling cells and the sample

size were suggested in a way that the so-called external error (the error of the DSMC method related to the quality and size of information sampled during the simulation) does not violate the prescribed value. Plotnikov and Shkarupa⁴⁰ also addressed the issue of selecting the computational parameters of the DSMC method and provided practical recommendations for evaluating the quantities involved in the expressions simultaneously with the calculation of the flow macro-parameters. In another work, Plotnikov and Shkarupa⁴¹ compared three statistical error evaluation approaches and found that they all provided reasonable results for the density and velocity and temperature estimates.

B. Type II incorrect acceptance error: premature initiation of sampling

As shown in the previous subsection, the type I (incorrect rejection) error was investigated comprehensively in many previous works; for example, Hadjiconstantinou *et al.*'s approach³⁵ based on the equilibrium statistical mechanics, and Plotnikov and Shkarupa's approach³⁸⁻⁴¹ based on the central limit theorem for the Markov processes. On the other hand, very few studies have been conducted on the type II (incorrect acceptance) error, in spite of its essential role in the effective and uninterrupted use of the DSMC method in complicated problems.

Bird^{3,23} developed the first automatic method for estimating steady state convergence based on the variation in the total number of simulated particles in the simulation domain. However, the method could not handle a flow with a constant number of particles, or highly unsteady regions, like recirculating flow. Burt and Boyd²⁶ developed a method that can resolve the insensitivity of Bird's method to weak transient behavior in local regions of relatively low density. The method was based on the variation in particle fluxes on the boundaries at two successive time-steps. The method was, however, found to suffer from an inability to deal with problems allowing scatter-induced fluctuations in the location of high gradient regions such as shock-boundary layer interaction.

Recently, Karchani *et al.*⁴² revisited the type II error and investigated in detail the effects of the incorrect inclusion of samples using the phase portraits of the sampling estimators and distribution of samples. The higher order phase portraits were found to provide the best illustration of the transition phase. Further, based on the observation that the Boltzmann collisional invariants are continuously changing in the unsteady phase, fully-automatic global and local steady state detection methods based on a probabilistic automatic reset sampling (PARS) were developed. The steady state method is based on a relative standard variation of collisional invariants, enabling it to be more sensitive to the momentum and energy variations during the unsteady phase. The method was shown to successfully handle the flows that are still evolving after the total number of particles had already reached an asymptotic value.

VI. Concluding remarks and outlook

The difficulty in studying the verification of solutions of the stochastic DSMC method lies in the unique features of the method: the pure simulation method is not based on any partial differential equations, and the stochastic Monte Carlo process is ubiquitously involved in the simulation. Another difficulty in developing a rigorous theory of the error estimation is the high degree of sampling data dependence, which is directly related to the high disparity in collision rates in the simulation domain.

Nonetheless, as shown in the present review, there has been substantial progress in the study of verification methods for the DSMC method in the last three decades, recently boosted by the rapid advance of computing power and software. Also, as the DSMC method is applied more and more frequently to challenging real-world problems of technical and industrial interest, verification studies of the method are expected to be increasingly important in the future.

To maximize the full potential of the DSMC method, pioneered by the late G. A. Bird, further research on some unsolved topics should be actively pursued. For example, improving the estimation of computational errors, and finding reference solutions, remain essential to the verification of the solutions and algorithms of the DSMC method. In the same context, developing error estimators for coarse cells and solution adaptations based on automated error estimation may be key to the effective application of the DSMC method to real-world problems. Further, the effects of various boundary conditions on the accuracy and convergence behavior of the DSMC method are also essential, as is the case with the CFD method, where the boundary condition has a direct impact on the accuracy of CFD. This problem will become more complicated when coupled with uncertainty residing in the treatment of collisions of gas molecules with solid wall atoms. Lastly, uncertainty quantification of model parameters introduced in the DSMC method will remain an important issue, in particular, in hypersonic flows with chemical reactions where large variability of reaction rates and wall catalysis may be present in the model.

Acknowledgments

The first author (R.S.M.) acknowledges the support from the National Research Foundation of Korea funded by the Ministry of Science and ICT (NRF 2017-R1A2B2007634), South Korea. The third author (O.E.) acknowledges the support provided by Korean Institute of Science and Technology Information (KISTI), South Korea.

References

- [1] G. A. Bird, "Approach to translational equilibrium in a rigid sphere gas," *Phys. Fluids* **6**, 1518 (1963).
- [2] G. A. Bird, *Molecular Gas Dynamics* (Clarendon, 1976).
- [3] G. A. Bird, *Molecular Gas Dynamics and the Direct Simulation of Gas Flows* (Oxford Science, 1994).

- [4] R. Zakeri, R. K. Moghadam, and M. Mani, “New chemical-DSMC method in numerical simulation of axisymmetric rarefied reactive flow,” *Phys. Fluids* **29**, 047105 (2017).
- [5] O. Tumuklu, V. Theofilis, and D. A. Levin, “On the unsteadiness of shock–laminar boundary layer interactions of hypersonic flows over a double cone,” *Phys. Fluids* **30**, 106111 (2018).
- [6] A. M. Mahdavi and E. Roohi, “Investigation of cold-to-hot transfer and thermal separation zone through nano step geometries,” *Phys. Fluids* **27**, 072002 (2015).
- [7] P. Wang, W. Su, and Y. Zhang, “Oscillatory rarefied gas flow inside a three dimensional rectangular cavity,” *Phys. Fluids* **30**, 102002 (2018).
- [8] M. A. Gallis, T. P. Koehler, J. R. Torczynski, and S. J. Plimpton, “Direct simulation Monte Carlo investigation of the Richtmyer-Meshkov instability,” *Phys. Fluids* **27**, 084105 (2015).
- [9] M. A. Gallis, N. Bitter, T. Koehler, J. Torczynski, S. Plimpton, and G. Papadakis, “Molecular-level simulations of turbulence and its decay,” *Phys. Rev. Lett.* **118**, 064501 (2017).
- [10] W. L. Oberkampf and C. J. Roy, *Verification and Validation in Scientific Computing* (Cambridge University Press, 2010).
- [11] R. S. Myong, “Thermodynamically consistent hydrodynamic computational models for high-Knudsen-number gas flows,” *Phys. Fluids* **11**, 2788 (1999).
- [12] N. T. P. Le, H. Xiao, and R. S. Myong, “A triangular discontinuous Galerkin method for non-Newtonian implicit constitutive models of rarefied and microscale gases,” *J. Comput. Phys.* **273**, 160 (2014).
- [13] A. Rana, R. Ravichandran, J. H. Park, and R. S. Myong, “Microscopic molecular dynamics characterization of the second-order non-Navier-Fourier constitutive laws in the Poiseuille gas flow,” *Phys. Fluids* **28**, 082003 (2016).
- [14] K. Nanbu, “Direct simulation scheme derived from the Boltzmann equation. II. Multicomponent gas mixtures,” *J. Phys. Soc. Japan* **49**, 2050 (1980).
- [15] K. Nanbu, “Interrelations between various direct simulation methods for solving the Boltzmann equation,” *J. Phys. Soc. Japan* **52**, 3382 (1983).
- [16] H. Babovsky and R. Illner, “A convergence proof for Nanbu’s simulation method for the full Boltzmann equation,” *SIAM J. Num. Anal.* **26**, 45 (1989).
- [17] W. Wagner, “A convergence proof for Bird’s direct simulation Monte Carlo method for the Boltzmann equation,” *J. Stat. Phys.* **66**, 1011 (1992).

- [18] E. Meiburg, “Comparison of the molecular dynamics method and the direct simulation Monte Carlo technique for flows around simple geometries,” *Phys. Fluids* **29**, 3107 (1986).
- [19] F. J. Alexander, A. L. Garcia, and B. J. Alder, “Cell size dependence of transport coefficients in stochastic particle algorithms,” *Phys. Fluids* **10**, 1540 (1998).
- [20] A. L. Garcia and W. Wagner, “Time step truncation error in direct simulation Monte Carlo,” *Phys. Fluids* **12**, 2621 (2000).
- [21] N. G. Hadjiconstantinou, “Analysis of discretization in the direct simulation Monte Carlo,” *Phys. Fluids* **12**, 2634 (2000).
- [22] M. A. Gallis, J. Torczynski, and D. Rader, “Molecular gas dynamics observations of Chapman-Enskog behavior and departures therefrom in nonequilibrium gases,” *Phys. Rev. E* **69**, 042201 (2004).
- [23] G. A. Bird, *Sophisticated DSMC* (Notes for DSMC07, Santa Fe, 2007).
- [24] G. A. Bird, M. A. Gallis, J. Torczynski, and D. Rader, “Accuracy and efficiency of the sophisticated direct simulation Monte Carlo algorithm for simulating noncontinuum gas flows,” *Phys. Fluids* **21**, 017103 (2009).
- [25] M. A. Gallis, J. Torczynski, D. Rader, and G. A. Bird, “Convergence behavior of a new DSMC algorithm,” *J. Comput. Phys.* **228**, 4532 (2009).
- [26] J. M. Burt and I. D. Boyd, “Convergence detection in direct simulation Monte Carlo calculations for steady state flows,” *Commun. Comput. Phys.* **10**, 807 (2011).
- [27] A. Karchani, and R. S. Myong, “Convergence analysis of the direct simulation Monte Carlo based on the physical laws of conservation,” *Comput. Fluids* **115**, 98 (2015).
- [28] E. Taheri, E. Roohi, and S. Stefanov, “On the convergence of the simplified Bernoulli trial collision scheme in rarefied Fourier flow,” *Phys. Fluids* **29**, 062003 (2017).
- [29] M. A. Gallis, J. Torczynski, D. Rader, M. Tij, and A. Santos, “Normal solutions of the Boltzmann equation for highly nonequilibrium Fourier flow and Couette flow,” *Phys. Fluids* **18**, 017104 (2006).
- [30] H. Akhlaghi, E. Roohi, and S. Stefanov, “On the consequences of successively repeated collisions in no-time-counter collision scheme in DSMC,” *Comput. Fluids* **161**, 23 (2018).
- [31] A. L. Garcia, “Nonequilibrium fluctuations studied by a rarefied-gas simulation,” *Phys. Review A* **34**, 1454 (1986).
- [32] M. Fallavollita, D. Baganoff, and J. McDonald, “Reduction of simulation cost and error for particle simulations of rarefied flows,” *J. Comput. Phys.* **109**, 30 (1993).
- [33] G. Chen and I. D. Boyd, “Statistical error analysis for the direct simulation Monte Carlo technique,” *J. Comput. Phys.* **126**, 434 (1996).

- [34] S. Rjasanow, T. Schreiber, and W. Wagner, "Reduction of the number of particles in the stochastic weighted particle method for the Boltzmann equation," *J. Comput. Phys.* **145**, 382 (1998).
- [35] N. G. Hadjiconstantinou, A. L. Garcia, M. Z. Bazant, and G. He, "Statistical error in particle simulations of hydrodynamic phenomena," *J. Comput. Phys.* **187**, 274 (2003).
- [36] H. M. Cave, K. C. Tseng, J. S. Wu, M. C. Jermy, J. C. Huang, and S. P. Krumdieck, "Implementation of unsteady sampling procedures for the parallel direct simulation Monte Carlo method," *J. Comput. Phys.* **227**, 6249 (2008).
- [37] Q. Sun, J. Fan, and I. D. Boyd, "Improved sampling techniques for the direct simulation Monte Carlo method," *Comput. Fluids* **38**, 475 (2009).
- [38] M. Y. Plotnikov and E. Shkarupa, "Estimation of the statistical error of the direct simulation Monte Carlo method," *Comput. Math. Math. Phys.* **50**, 335 (2010).
- [39] M. Y. Plotnikov and E. Shkarupa, "Some approaches to error analysis and optimization of the DSMC method," *Russ. J. Numer. Anal. Math. M.* **25**, 147 (2010).
- [40] M. Y. Plotnikov and E. Shkarupa, "Theoretical and numerical analysis of approaches to evaluation of statistical error of the DSMC method," *Comput. Fluids* **105**, 251 (2014).
- [41] M. Y. Plotnikov and E. V. Shkarupa, "Selection of sampling numerical parameters for the DSMC method," *Comput. Fluids* **58**, 102 (2012).
- [42] A. Karchani, O. Ejtehadi, and R. S. Myong, "A probabilistic automatic steady state detection method for the direct simulation Monte Carlo," *Commun. Comput. Phys.* **20**, 1183 (2016).